Study of a dual frequency atmospheric pressure corona plasma

Dan Bee Kim, S. Y. Moon, H. Jung, B. Gweon, and Wonho Choe

Related Articles

Sheath structure in negative ion sources for fusion (invited)
Rev. Sci. Instrum. 83, 02B109 (2012)

A close-coupling multi-antenna type radio frequency driven ion source
Rev. Sci. Instrum. 83, 02B106 (2012)

Design and fabrication of a superconducting magnet for an 18 GHz electron cyclotron resonance ion/photon source NFRI-ECRIPS
Rev. Sci. Instrum. 83, 02A326 (2012)

Plasma resonances in a microwave-driven microdischarge
Appl. Phys. Lett. 100, 064102 (2012)

Off-line ionization tests using the surface and the plasma ion sources of the SPES project
Rev. Sci. Instrum. 83, 02A907 (2012)

Additional information on Phys. Plasmas

Study of a dual frequency atmospheric pressure corona plasma

Dan Bee Kim,[a)] S. Y. Moon,[b)] H. Jung, B. Gweon, and Wonho Choe[c)]
Department of Physics, Korea Advanced Institute of Science and Technology, 335 Gwahangno, Yuseong-gu, Daejeon 305-701, Republic of Korea

Radio frequency mixing of 2 and 13.56 MHz was investigated by performing experimental measurements on the atmospheric pressure corona plasma. As a result of the dual frequency, length, current density, and electron excitation temperature of the plasma were increased, while the gas temperature was maintained at roughly the same level when compared to the respective single frequency plasmas. Moreover, observation of time-resolved images revealed that the dual frequency plasma has a discharge mode of 2 MHz positive streamer, 2 MHz negative glow, and 13.56 MHz continuous glow. © *2010 American Institute of Physics*. [doi:10.1063/1.3430636]

I. INTRODUCTION

Atmospheric pressure corona discharges have been widely applied to various fields. Recently, together with the typical frequency range of dc to low frequency (LF: several tens of kilohertz), 13.56 MHz radio frequency corona discharges have been actively employed in bio and chemical applications.[1–6] Nevertheless, a comparative study on different driving frequency ranges has yet to be performed thoroughly, despite the fact that the driving frequency is one of the important parameters controlling the discharge nature. A previous study by the authors investigated the corona plasmas driven by two driving frequency ranges, LF and rf, and defined the discharge characteristics at each range.[7]

We found that each frequency range induces distinctive discharge features. For instance, rf is favorable for its low breakdown voltage and high plasma density, and the rf field produces a continuous discharge unlike the LF plasma, the discharge of which has a pulselike nature due to space charge accumulation. The high density and temperature of the rf plasma may enhance the application efficiency on the one hand, but its heat and current may cause detrimental effects to sensitive targets such as living organisms on the other hand. Meanwhile, since the streamer, which carries very highly energetic ions and electrons and thus plays a key role in some applications such as surface treatment,[8] involves ion motion, only corona plasma driven by a driving frequency under 2 MHz exhibits this mode. Also, the longer length of the LF plasma can broaden the accessibility to the treatment target. Thus, the frequency ranges of LF and rf, respectively, have unique characteristics. For this reason, we attempted frequency mixing in the present work.

In low pressure capacitively coupled plasma (CCP), the dual frequency concept was introduced to independently control the ion flux and energy, and it has been widely studied since and applied practically in the industry.[9–11] Our group has investigated the driving frequency effects in atmospheric pressure CCP, including a dual frequency study.[12,13]

The dual frequency experiment is still in progress, but it has been found that the addition of 2 MHz power enlarged the abnormal glow regime for 13.56 MHz plasma by lowering the required power for the plasma to fill the entire electrode area.

In the present study, 2 MHz was mixed with 13.56 MHz. It was anticipated that if the mixing frequency resulted in coexistence of the efficient streamer mode of long length found at driving frequency less than 2 MHz and the 13.56 MHz continuous glow mode of high density and temperature, then a plasma having all the features originating from each input frequency could be derived. The basic properties of the dual frequency plasma were investigated and compared with those of single frequency plasmas to identify the effects of the dual frequency.

II. EXPERIMENTS

A simple schematic of the plasma system is illustrated in Fig. 1(a). Basically, it consists of a copper pin electrode and a Pyrex glass tube. A detailed description of the plasma source used in the experiment can be found in our previous report.[7] We supplied 2 MHz power using a function generator (Marconi 2023), an amplifier (AR 500A100A), an impedance matcher, and a 13.56 MHz resonance filter. 13.56 MHz power (Dressler Cesar 1312) was supplied through an impedance matcher. Both powers were applied to the copper pin electrode, and the plasma was produced under a helium gas supply at 3 l/min in the ambient air. The discharge voltage and current were measured using a VI probe (ProSys). A time-resolved (wavelength unresolved) plasma image was obtained using an intensified charge coupled device (ICCD) camera (Princeton Instrument-MAX2). The plasma emission spectrum was obtained by a spectrometer (Chromex 250is, wavelength range of 300–800 nm). The gas temperature was measured using a fiber thermometer (FISO FOT-H).

III. RESULTS AND DISCUSSIONS

Figure 1 presents the plasma images taken by a CCD camera for the single frequency cases of (b) 2 MHz and (c) 13.56 MHz both at an input power (P_{in}) of 75 W and for the dual frequency case of (d) 2 and 13.56 MHz at a total P_{in}

---
a)Present address: Korea Research Institute of Standards and Science.
b)Present address: LG Electronics Advanced Research Institute.
c)Author to whom correspondence should be addressed. Electronic mail: wchoe@kaist.ac.kr.
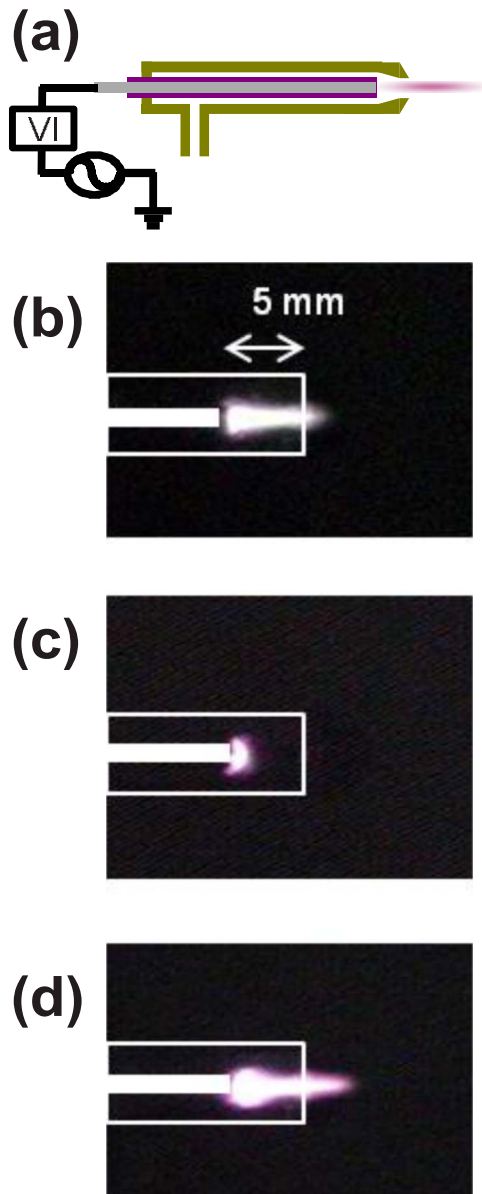
(a)

(b)

5 mm

(c)

(d)

FIG. 1. (Color online) (a) Schematic of the plasma source and plasma images for single frequency of (b) 2 MHz and (c) 13.56 MHz, both at $P_{in}=75$ W, and for dual frequency of (d) 2 MHz+13.56 MHz at a total $P_{in}=150$ W (75 W each).
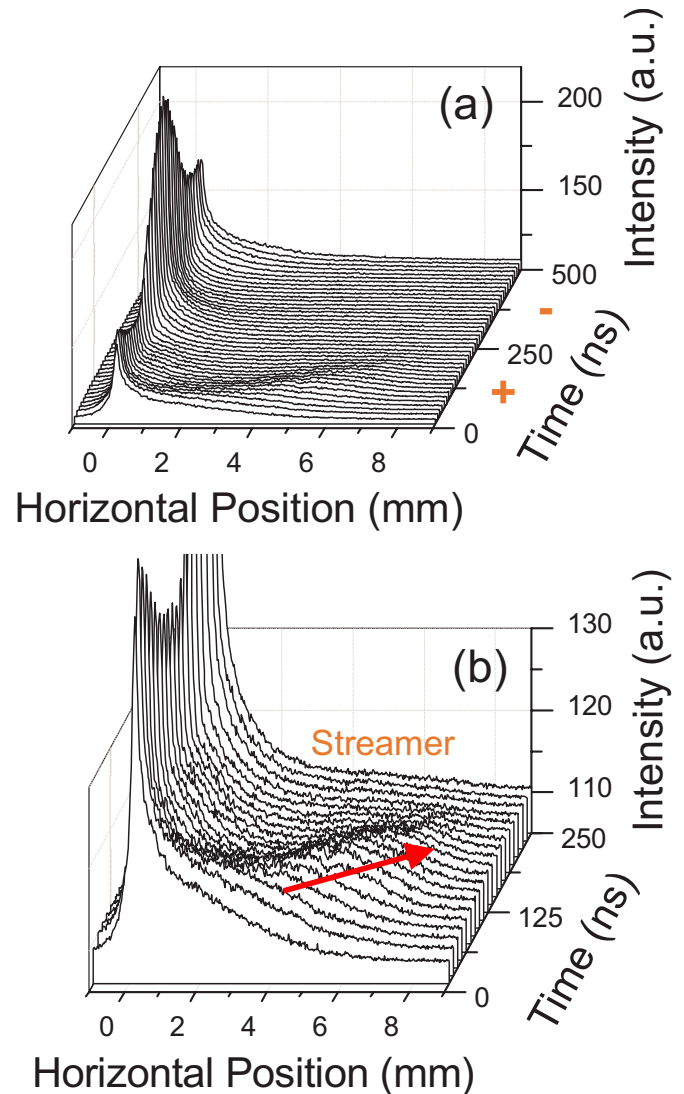

FIG. 2. (Color online) 3D plot for a time-resolved image of the dual frequency plasma and (b) zoom in of the plot for the positive period at a total $P_{in}=150$ W (75 W each).

of 150 W (75 W each). The dual frequency plasma was spherical near the electrode and cylindrical at some distance from the electrode, showing the appearance of a combination of the two single frequency plasmas. The 2 MHz plasma is originally almost three times longer in length (6 mm) than the 13.56 MHz plasma (2 mm). The difference in the plasma length for the different input frequency was previously observed, and it was explained by using an equation for the electron displacement, which is a function of the external electric field and input frequency.[7] When the plasma length is plotted against the discharge voltage, a linear relationship is obtained. Thus, it is found that in order to make the plasma length longer, the lower frequency is favorable, as its voltage is larger for the same power.[7,12] When the two frequencies were mixed, the plasma was lengthened by a few millimeters (26%) compared to the 2 MHz plasma even when the total

P_{in} was the same (7–9 mm at total $P_{in}=150$ W, 75 W each).

In order to confirm the temporal behavior of the discharge, a time-resolved plasma image was taken using an ICCD camera. The time-resolved dual frequency plasma image was transferred to a three-dimensional (3D) graph, as presented in Fig. 2. Here, the x axis represents the horizontal position parallel to the electrode, and the y axis and the z axis correspond to the time and intensity of the plasma image, respectively. A pin electrode is placed at the horizontal position of 0 mm. The period of 2 MHz is 500 ns, and the first 250 ns corresponds to a half period with positive voltage, shown in Fig. 2(a). Overall, the plasmas of each half period are in different discharge modes, namely, the positive (voltage) streamer and the negative (voltage) glow. Figure 2(b), presenting a zoom in of the positive period, clearly shows the streamer propagation. During the negative period, the plasma was confined near the pin electrode as the glow mode. Such asymmetry originates from the difference in the mobility of the space charge for each half period in the asymmetric source geometry.[7,14] Another time-resolved measurement

employing a photomultiplier tube indicated the presence of the 13.56 MHz glow at the pin electrode. Therefore, the dual frequency plasma has both 2 and 13.56 MHz discharge modes simultaneously.

The slope of the 2 MHz power I-V curve showed little change (decreased by 10%) with the addition of 13.56 MHz power, compared to the 2 MHz single frequency case. Since the plasmas have different volumes, the volume current density ($=I_{rms}$/volume [A/mm^3]) was calculated and plotted in Fig. 3(a) for a fair comparison. The discharge volume was roughly estimated. For the dual frequency plasma, based on the plasma image, we divided the plasma into two sections of sphere and cylinder. By counting the pixels, the actual dimensions were gotten. This error is between 10% and 15%. Then, the volumes of the sphere and the cylinder were each calculated and added to obtain the total discharge volume. In case of 2 and 13.56 MHz plasmas, each was seen as cylinder and sphere, respectively. It can be seen that the total current density of the dual frequency plasma (-▲-) is increased by as much as three times for the same discharge voltage, indicating the electron density and/or temperature increment.[15] For the reference, the power density range of the 13.56 MHz plasma (-□-) is more than twofold higher, as shown in Fig. 3(a).

Three representative molecular/atomic emission lines of N_2^+ (391.4 nm), He I (706.5 nm), and O I (777.5 nm) were observed. The measurement was made using a spectrometer and an optical fiber placed at about 30 mm from the pin electrode at the same axis. Line integrated emission was obtained. N_2^+ is excited by low energy electrons (excitation of N_2^+ by 3 eV electrons) while the helium excitation requires higher energy electrons of 22 eV (ground state electron impact excitation), respectively.[16] Hence, each spectral line may represent the behavior of low and high energy electrons. For the same volume power density, the N_2^+ intensity normalized to He I was increased by as much as roughly 1.5 times for the dual frequency plasma compared to the 2 MHz plasma, as shown in Fig. 3(b). Although He I was also increased, it means that the N_2^+ increment was larger. It seems like there are more of the low energy electrons than the high energy ones, and one of the reasons may be attributed to the fact that the electrons can transfer their energy more efficiently to the heavy particles with the volume expansion.[17] Furthermore, the O I intensity, one of the oxygen radicals, was also increased like N_2^+. The oxygen radicals play a key role in some applications such as the bioapplications. Meanwhile, the N_2^+ intensity of the 13.56 MHz plasma in Fig. 3(b) shows the opposite behavior. It may be coming from the fact that the single 13.56 MHz plasma is confined in the glass tube, and there is relatively less introduction of air molecules to the plasma, thus, lower nitrogen and oxygen line intensities.

At atmospheric pressure, the electron excitation temperature (T_{exe}) indicates the tendency of the electron temperature, as it is considered as the minimum value.[18,19] T_{exe} was measured based the well-known Boltzmann plot method using He I atomic emission lines (587.6, 667.8, 706.52, and 728.14 nm).[20] For the same power density, T_{exe} of the dual frequency plasma was larger than that of the 2 MHz plasma,
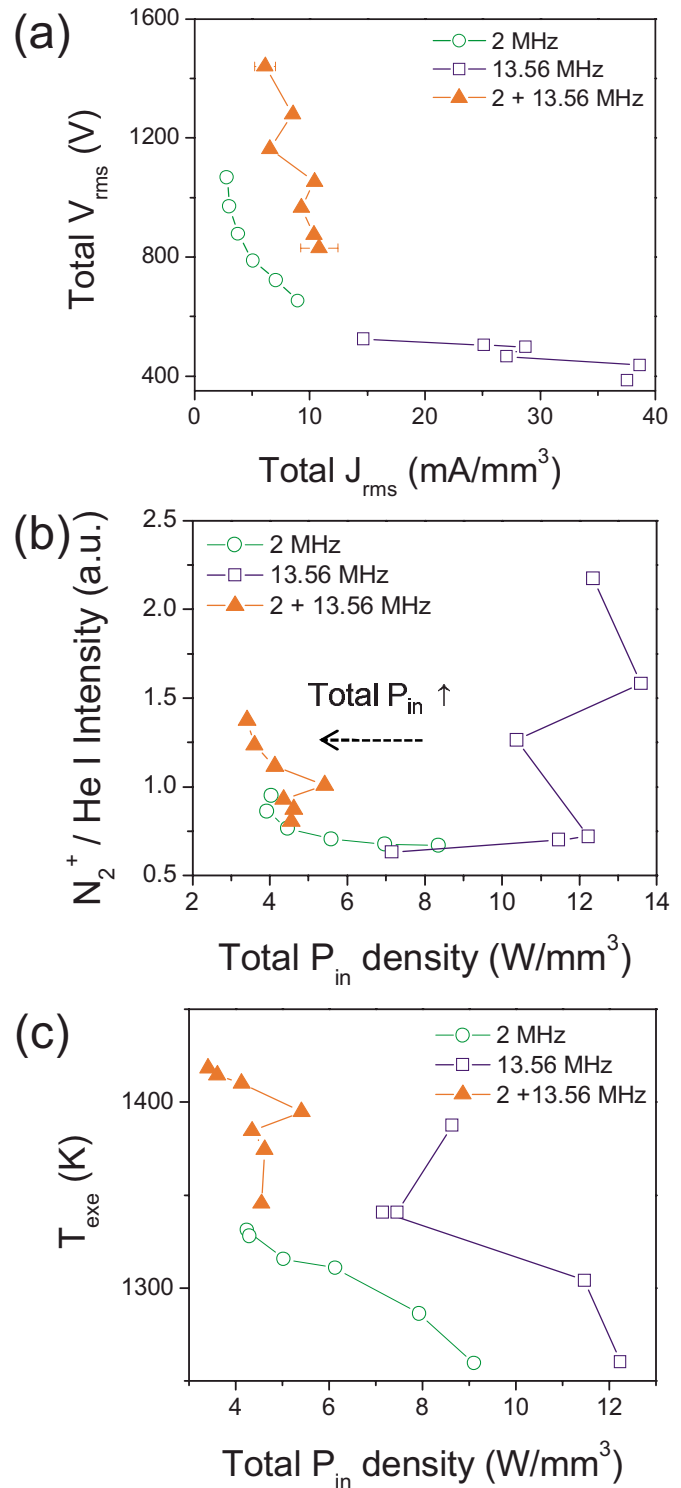

FIG. 3. (Color online) (a) Total volume current density vs voltage curve. (b) N_2^+ (391.4 nm) intensity normalized to He I (706.5 nm) for total volume power density. The total P_{in} density was decreased as the total P_{in} was increased due to the discharge volume expansion. The dotted arrow in the plot shows the total P_{in} increase direction. (c) T_{exe} vs total volume power density. For the dual frequency case, the 2 MHz P_{in} was varied from 10 to 100 W while the 13.56 MHz P_{in} was fixed at 75 W.

and it was still larger than the 13.56 MHz plasma with the higher power density as depicted in Fig. 3(c). The high ratio of electron to gas temperature may reflect higher chemical reaction efficiency, as little power is consumed in the gas heating.
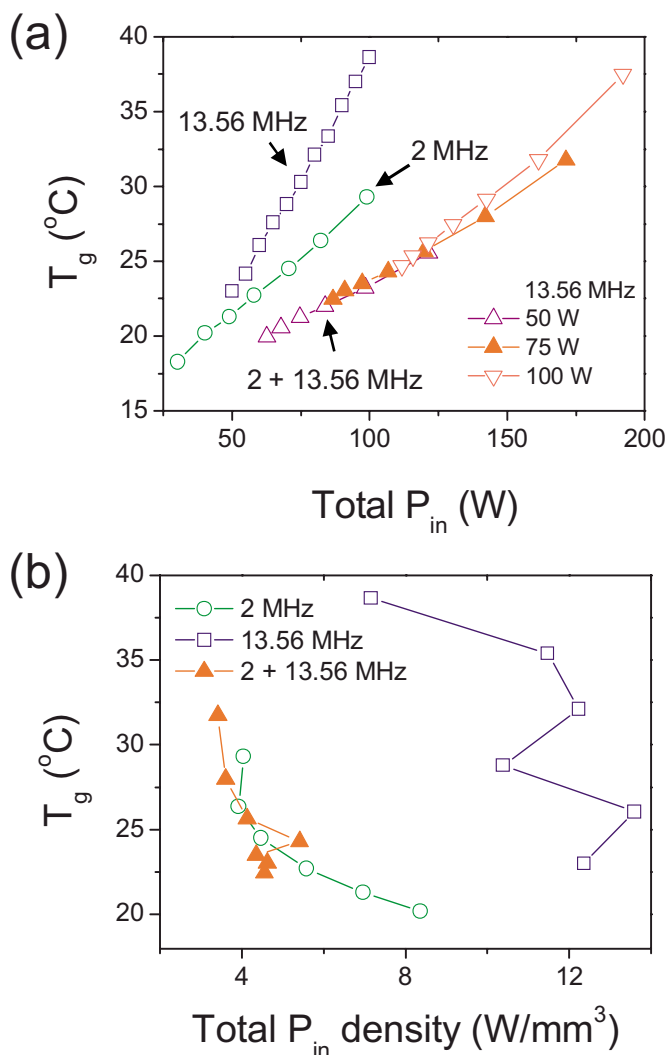
FIG. 4. (Color online) (a) T_g vs total input power and (b) total volume input power density. For the dual frequency case, 13.56 MHz P_{in} was fixed at (-△-) 50 W, (-▽-) 75 W, and (-▲-) 100 W, respectively.

The gas temperature (T_g) was measured using a fiber thermometer placed at about 2.5 mm from the pin electrode. Although the thermometer was injected in the plasma, its dielectric nature did not affect the plasma much. T_g of the 13.56 MHz plasma is higher than that of the 2 MHz plasma for the same total P_{in}, as described in Fig. 4(a). The higher gas temperature results from the 13.56 MHz discharge being rather continuous whereas the 2 MHz discharge is pulselike. Also, the discharge volume is smaller for the 13.56 MHz case. For the dual frequency case, T_g was as much as 7 °C lower with respect to the 2 MHz plasma for the same total P_{in}. The gas cools down as the discharge volume expands, so with the increase in the discharge volume, T_g of the dual frequency plasma can be lower. Yet again, upon considering the different plasma volume, T_g was assessed according to the volume power density [Fig. 4(b)]. The total power is higher where the power density is low because this plasma volume is expanded with the increase in P_{in}. With the addition of the 13.56 MHz power or with the increase in the 2 MHz power itself, the electrons gain more energy, and they heat up the gas by transferring energy through collisions. At the same time, the gas cools down with the volume expansion. With the volume expansion, however, the electrons can transfer their energy to the heavy particles more efficiently.[17] Namely, there is competition between the electron induced gas heating and the volume expansion gas cooling, and in our case, the gas heating seems to become more dominant than the gas cooling as more power is added. Hence, at the higher total P_{in}, the gas temperature is higher even with the lower power density because the electrons transfer energy to the heavy particles more efficiently. Nonetheless, the gas temperature of the dual frequency plasma was almost the same with the single 2 MHz plasma for the same power density, and keeping the gas temperature low is important for certain applications such as heat sensitive biomaterial treatments.

IV. SUMMARY

In summary, mixing two rfs of 2 and 13.56 MHz lengthened the plasma and increased its current density and electron excitation temperature while the gas temperature was retained at roughly the same level when compared with the respective single frequency plasmas. In addition, it was found that the dual frequency plasma has discharge modes of both 2 and 13.56 MHz, namely, 2 MHz negative glow and positive streamer and 13.56 MHz continuous glow. The increased plasma length enlarges the application range because the interelectrode distance, which affects both density and temperature of the plasma, can be varied over a larger range. Also, the higher electron density and temperature (inferred from the increase in the current density and the electron excitation temperature) and the higher ratio of electron to gas temperature suggests more efficient plasma chemical reactions. The 2 and 13.56 MHz dual frequency atmospheric pressure corona plasma uniformly showed superior discharge characteristics.

[1] A. Shashurin, M. Keidar, S. Bronnikov, R. A. Jurjus, and M. A. Stepp, Appl. Phys. Lett. **93**, 181501 (2008).
[2] E. Stoffels, I. E. Kieft, and R. E. J. Sladek, J. Phys. D: Appl. Phys. **36**, 2908 (2003).
[3] D. B. Kim, B. Gweon, S. Y. Moon, and W. Choe, Curr. Appl. Phys. **9**, 1093 (2009).
[4] B. Gweon, D. B. Kim, S. Y. Moon, and W. Choe, Curr. Appl. Phys. **9**, 625 (2009).
[5] H. P. Song, B. Kim, J. H. Choe, S. Jung, S. Y. Moon, W. Choe, and C. Jo, Food Microbiol. **26**, 432 (2009).
[6] H. Jung, D. B. Kim, B. Gweon, S. Y. Moon, and W. Choe, Appl. Catal., B **93**, 212 (2010).
[7] D. B. Kim, J. K. Rhee, B. Gweon, S. Y. Moon, and W. Choe, Appl. Phys. Lett. **91**, 151502 (2007).
[8] M. Goldman, A. Goldman, and R. S. Sigmond, Pure Appl. Chem. **57**, 1353 (1985).
[9] P. C. Boyle, A. R. Ellingboe, and M. M. Turner, J. Phys. D: Appl. Phys. **37**, 697 (2004).
[10] W. Tsai, G. Mueller, R. Lindquist, B. Frazier, and V. Vahedi, J. Vac. Sci. Technol. B **14**, 3276 (1996).
[11] E. Cianci, A. Schina, A. Minotti, S. Quaresima, and V. Foglietti, Sens. Actuators, A **127**, 80 (2006).

[12] S. Y. Moon, D. B. Kim, B. Gweon, and W. Choe, Appl. Phys. Lett. **93**, 221506 (2008).

[13] S. Y. Moon, Proceedings of the Ninth Asia-Pacific Conference On Plasma Science and Technology (APCPST) and 21st Symposium On Plasma Science for Materials (SPSM), Huangshan, China, 2008.

[14] D. B. Kim, J. K. Rhee, S. Y. Moon, and W. Choe, Appl. Phys. Lett. **89**, 061502 (2006).

[15] E. Amanatides and D. Mataras, J. Appl. Phys. **89**, 1556 (2001).

[16] D. W. Liu, F. Iza, and M. G. Kong, Appl. Phys. Lett. **95**, 031501 (2009).

[17] E. Stoffels, A. J. Flikweert, W. W. Stoffels, and G. M. W. Kroesen, Plasma Sources Sci. Technol. **11**, 383 (2002).

[18] J. A. M. van der Mullen, Phys. Rep. **191**, 109 (1990).

[19] A. Sola, M. D. Calzada, and A. Gamero, J. Phys. D **28**, 1099 (1995).

[20] W. Lochte-Holtgreven, *Plasma Diagnostics* (North-Holland, Amsterdam, 1968), Chaps. 1 and 3.